Modelling and Experimental Validation of Articulated Mobile Robots with Hybrid Locomotion System

Modelling and experimental validation of articulated mobile robots with hybrid locomotion system

Andrea Botta, Paride Cavallone, Luca Carbonari,
Luigi Tagliavini and Giuseppe Quaglia

Politecnico di Torino, Italy
{andrea.botta, paride.cavallone,luca.carbonari,
luigi.tagliavini, giuseppe.quaglia}@polito.it

Abstract. In recent years, autonomous vehicles and mobile robots are starting to become a trend also in several new fields of application. In some cases, they are articulated vehicles with an active front module and a rear one that is pulled passively or that can contribute to the vehicle traction when required. Although modelling of mobile robots is not a novelty, most of the available studies are limited to kinematic or very basic dynamic models. In order to correctly simulate mobile robots with fast dynamics or operating off-road, this study proposes a dynamic model of such systems derived taking into account lateral and longitudinal slip in the wheels. The model is then validated experimentally using a small articulated robot

Keywords: Mobile robot, Articulated robots, Tractor-trailer.

1 Introduction

The application of mobile robots is growing interest in many fields of application, and in recent decades various mobile platforms have been designed to achieve even various tasks. In parallel to the development of new mobile robots, researchers have proposed several models of increasing complexity in order to describe and predict how a robot, or a class of robots, should behave and to design an optimal controller.

The modelling of such systems is not new, and many works have focused on the main type of mobile robots composed by a single module such as differential drive [1] or car-like robots [2]. Fewer studies go into detail about multi-modular vehicle, but, thanks to some interest in developing autonomous trucks, there are some researches about modelling articulated (or tractor-trailer) robots, but most of the knowledge comes from studies about conventional vehicles [3–7]. Although these studies can provide some insight about how mobile articulated robots can behave, most of them are limited to just kinematic or to dynamic models with rigorous hypotheses. Therefore these models are not suited to describe robots having very fast dynamics or operating off-road or, more in general, in conditions where significant longitudinal or lateral wheel slips can occur.

This paper intends to develop a dynamic model of a generic articulated robot composed of two modules having four wheels, where each module can work as a differential drive device. This necessity came from the need of modelling two mobile robots with a similar architecture: Agri.Q, an Unmanned Ground Vehicle (UGV) designed for precision agriculture [8–10], and Epi.Q, a modular surveillance UGV [11–15](Fig. 1).

Ideally, the same model could be developed for them and, even more generally, in order to represent articulated robots with more than two modules and different locomotion units, like for Rese.Q a snake-like tracked robot [16, 17].

Fig. 1. Agri.Q and Epi.Q, UGVs composed of two differential driven modules linked together.

2 System modelling

The system that is analysed and modelled is a generic mobile robot made of two modules with four wheels that can be independently actuated or not. With this architecture, it is possible to get several combinations such as the front module pulling the second one like a trailer, the second one pushing the first robot unit or both modules working together.

A schematic model of the system is illustrated in Fig. 2. In this figure, the first platform has its mass m_1 centred at the point F, while point R represents the second module of mass m_2. The two modules are linked by the two links L_1 and L_2 joined together by a passive revolute joint at the point O to establish a relative yaw motion between the modules. Although in the actual robots there is also a joint enabling the relative roll motion, the model does not represent it, since it is limited to the planar movement. For the generic module $j = 1,2$, it is possible to locate the four wheels of mass m_{jk} at $(\pm d_j, \pm b_j)$ in the local reference frame placed at the module centre of mass.

The two robot robots introduced before, Agri.Q and Epi.Q, can be easily represented by this model changing the appropriate geometric and mass parameters and adding some more constraints on the wheels to correctly represents the specific locomotion unit.

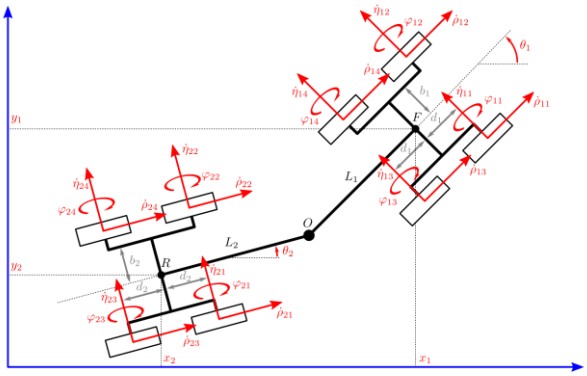

Fig. 2. Dynamic model generalised coordinates and geometric parameters.

Table 1 collects the states of the system required to represent the robot, which are repeated for each module and each wheel: three coordinates (x_j, y_j, θ_j) define the pose of each module and other three coordinates $(\rho_{jk}, \eta_{jk}, \varphi_{jk})$ describe the state of each wheel. Therefore, given two modules and eight wheels, it is possible to define the generalised coordinates vector $\mathbf{q}_{30\times1}$ collecting all of them.

Table 1. Generalised coordinates description

Symbol	*Description*
j	Module subscript. It is 1 or F for the front module and 2 or R for the rear one
k	Wheel subscript. Odd k is used for the right side, while even k for the left one
x_j	Horizontal position of the module j in the inertial reference frame
y_j	Vertical position of the module j in the inertial reference frame
θ_j	Heading of the module j in the inertial reference frame
η_{jk}	Lateral displacement of the wheel jk in the local reference frame
ρ_{jk}	Longitudinal displacement of the wheel jk in the local reference frame
φ_{jk}	Angular displacement of the wheel jk about its axis

However, the actual minimum number of states required to define the system adequately is 12: two spatial coordinates to define the position of a module in the plane, two angular coordinates to represent the heading of the modules and eight angular coordinates to represent the rotation of the wheels. Consequently, given the 30 states defined before, 18 constraint equations must be defined:

$$\dot{\rho}_{jk} = \dot{x}_j cos\theta_j + \dot{y}_j sin\theta_j - (-1)^k b_j \dot{\theta}_j \quad \text{with } j = 1,2 \text{ and } k = 1,2,3,4 \tag{1}$$

$$\dot{\eta}_{jk} = -\dot{x}_j sin\theta_j + \dot{y}_j cos\theta_j + d_j \dot{\theta}_j \quad \text{with } j = 1,2 \text{ and } k = 1,2 \tag{2}$$

$$\dot{\eta}_{jk} = -\dot{x}_j sin\theta_j + \dot{y}_j cos\theta_j - d_j \dot{\theta}_j \quad \text{with } j = 1,2 \text{ and } k = 3,4 \tag{3}$$

$$\dot{x}_2 = \dot{x}_1 + L_1\dot{\theta}_1 sin\theta_1 + L_2\dot{\theta}_2 sin\theta_2 \tag{4}$$

$$\dot{y}_2 = \dot{y}_1 - L_1\dot{\theta}_1 cos\theta_1 - L_2\dot{\theta}_2 cos\theta_2 \tag{5}$$

Where (1), (2), and (3) represent the longitudinal and lateral wheels slips, while (4) and (5) embodies the relationship between the front and rear modules. These constraints can be compactly written in matrix form defining the system constraint matrix $\mathbf{A}(\mathbf{q})$

$$\mathbf{A}_{18\times30}(\mathbf{q})\dot{\mathbf{q}}_{30\times1} = 0 \tag{6}$$

The Newton-Euler approach is used to derive the dynamic equations governing the system. The system is divided into 10 subsystems (front module, rear module and 8 wheels) and for each one of them a free body diagram is drawn (Fig. 3).

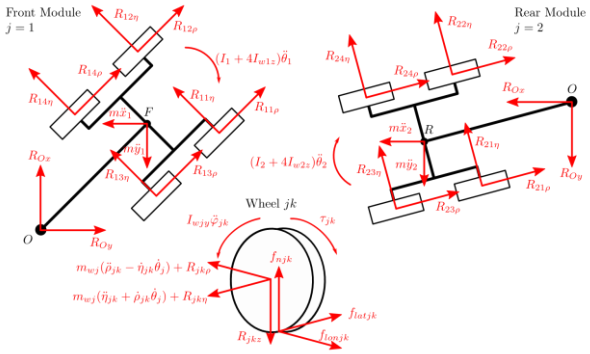

Fig. 3 Two modules and the generic wheel *jk* free-body diagrams

From the free-body diagrams in Fig. 3, it is possible to write down the three equations governing the first ($j = 1$) and the second module ($j = 2$):

$$m_j\ddot{x}_j = cos\theta_j \sum_{k=1}^{4} R_{jk\rho} - sin\theta_j \sum_{k=1}^{4} R_{jk\eta} - (-1)^j R_{Ox} \tag{7}$$

$$m_j\ddot{y}_j = sin\theta_j \sum_{k=1}^{4} R_{jk\rho} + cos\theta_j \sum_{k=1}^{4} R_{jk\eta} - (-1)^j R_{Oy} \tag{8}$$

$$\begin{aligned} &(I_j + 4I_{wjz})\ddot{\theta}_j = \\ &= b_j \sum_{k=1}^{4} (-(-1)^k R_{jk\rho}) + d_j(R_{j1\eta} + R_{j2\eta} - R_{j3\eta} - R_{j4\eta}) + L_j(R_{Ox}sin\theta_j - R_{Oy}cos\theta_j) \end{aligned} \tag{9}$$

To complete the dynamic equations of the system, a set of three equations can be defined for the generic wheel jk with $j = 1,2$ and $k = 1,2,3,4$. As said before, the

vertical dynamics are neglected, and the normal force is just used to define the rolling resistance. The actual value of the normal force is the same for all the wheels.

$$m_{wj}\ddot{\rho}_{jk} = f_{lonjk} - R_{jk\rho} + m_{wj}\dot{\eta}_{jk}\dot{\theta}_j \tag{10}$$

$$m_{wj}\ddot{\eta}_{jk} = f_{latjk} - R_{jk\eta} - m_{wj}\dot{\rho}_{jk}\dot{\theta}_j \tag{11}$$

$$I_{wj}\ddot{\varphi}_{jk} = \tau_{jk} - r_{wj}f_{lonjk} - k_{rollj}f_{njk}\text{sign}(\dot{\varphi}_{jk}) \tag{12}$$

The set of 30 dynamic equations describing the system can be written in the following form:

$$\mathbf{M}\ddot{\mathbf{q}}\mathbf{f}(\dot{\mathbf{q}}) + \mathbf{C}(\mathbf{q},\dot{\mathbf{q}}) + \mathbf{f}(\dot{\mathbf{q}}) + \mathbf{A}(\mathbf{q})^{\mathrm{T}}\mathbf{R} = \mathbf{B}\boldsymbol{\tau} \tag{13}$$

Where $\mathbf{M}_{30\times30}$ is the diagonal mass matrix, due to the full kinematic decoupling of the states, $\mathbf{B}_{30\times8}$ is the input matrix, $\boldsymbol{\tau}_{8\times1} = \left[\tau_{11}, \dots, \tau_{jk}, \dots, \tau_{24}\right]^T$ is the input vector containing all the torques applied to the wheels, $\mathbf{f}(\dot{\mathbf{q}})_{30\times1}$ is the vector of the wheel-ground contact forces, $\mathbf{C}(\mathbf{q},\dot{\mathbf{q}})_{30\times1}$ is the Coriolis and centripetal forces vector, $\mathbf{A}(\mathbf{q})_{18\times30}$ is the system constraint matrix and $\mathbf{R}_{18\times1}$ is the constrain forces vector, or the Lagrange multipliers vector.

From (6) it can be derived that all the permitted velocities are in the null space of $\mathbf{A}(\mathbf{q})$. The null space can be represented by a set of vectors $\mathbf{n}_1(\mathbf{q}), \dots, \mathbf{n}_{12}(\mathbf{q})$ defining the base of the null space matrix of $\mathbf{A}(\mathbf{q})$:

$$\mathbf{A}(\mathbf{q})\mathbf{n}_{\mathrm{i}}(\mathbf{q}) = 0 \quad \text{with } i = 1,2,\dots,12 \tag{14}$$

So it is possible to define $\mathbf{N}(\mathbf{q})$ as the null space matrix of $\mathbf{A}(\mathbf{q})$ such as

$$\mathbf{A}_{18\times30}(\mathbf{q})\mathbf{N}_{30\times12}(\mathbf{q}) = 0 \Rightarrow \mathbf{N}(\mathbf{q})^{\mathrm{T}}\mathbf{A}(\mathbf{q})^{\mathrm{T}} = 0 \tag{15}$$

At the same time $\dot{\mathbf{q}}$ is a linear combination of the 12 vectors composing $\mathbf{N}(\mathbf{q})$, so it can be compactly written as $\dot{\mathbf{q}} = \mathbf{N}(\mathbf{q})\mathbf{u}$**.** Where $\mathbf{u}$ is a vector containing the minimum number of independent kinematic inputs $u_1, u_2, \dots, u_{12}$ needed to describe the system completely. For the general case proposed here, the vector of independent kinematics input of the system can be the as it follows:

$$\mathbf{u}_{12\times1} = \left[\dot{x}_1, \dot{y}_1, \dot{\theta}_1, \dot{\varphi}_{11}, \dot{\varphi}_{12}, \dot{\varphi}_{13}, \dot{\varphi}_{14}, \dot{\theta}_2, \dot{\varphi}_{21}, \dot{\varphi}_{22}, \dot{\varphi}_{23}, \dot{\varphi}_{24}\right]^T \tag{16}$$

Hence, it is possible to compute $\mathbf{N}(\mathbf{q})$ from $\mathbf{A}(\mathbf{q})$. With this new matrix, it is possible to redefine (13) using the minimum number of states following these steps:

$$\ddot{\mathbf{q}} = \dot{\mathbf{N}}\mathbf{u} + \mathbf{N}\dot{\mathbf{u}} \tag{17}$$

$$\mathbf{N}^{\mathrm{T}}\left(\mathbf{M}\dot{\mathbf{N}}\mathbf{u} + \mathbf{M}\mathbf{N}\dot{\mathbf{u}}\right) = \mathbf{N}^{\mathrm{T}}\mathbf{B}\boldsymbol{\tau} - \mathbf{N}^{\mathrm{T}}\mathbf{f} - \mathbf{N}^{\mathrm{T}}\mathbf{C} - \mathbf{N}^{\mathrm{T}}\mathbf{A}^{\mathrm{T}}\mathbf{R}$$

$$\mathbf{N}^{\mathrm{T}}\mathbf{M}\mathbf{N}\dot{\mathbf{u}} = \mathbf{N}^{\mathrm{T}}\mathbf{B}\boldsymbol{\tau} - \mathbf{N}^{\mathrm{T}}(\mathbf{M}\dot{\mathbf{N}}\mathbf{u} - \mathbf{C} - \mathbf{f})$$

$$\dot{\mathbf{u}} = \mathbf{H}\boldsymbol{\tau} - \mathbf{G}$$
$$\text{where } \mathbf{H} = (\mathbf{N}^{\mathrm{T}}\mathbf{M}\mathbf{N})^{-1}\mathbf{N}^{\mathrm{T}}\mathbf{B} \text{ and } \mathbf{G} = (\mathbf{N}^{\mathrm{T}}\mathbf{M}\mathbf{N})^{-1}\mathbf{N}^{\mathrm{T}}(\mathbf{M}\dot{\mathbf{N}}\mathbf{u} - \mathbf{f} - \mathbf{C}) \tag{18}$$

2.1 Contact forces

In order to correctly model the dynamics of a generic articulated system, the contact forces generated by the wheel-ground interaction are crucial. Most of the studies that consider slip and skid of the wheels use the Pacejka magic formula to model the contact forces. Unfortunately, the number of parameters required to model the contact is high and usually it is not easy to identify them if the wheels are not commercial tires. For this reason, a simpler model based on wheel normal, longitudinal and lateral stiffness is defined and used.

The normal contact force f_{njk} is defined as a linear function of the wheel normal displacement Δz_{jk}:

$$f_{njk} = k_{nj}\Delta z_{jk} \tag{19}$$

Again, in this preliminary model, the robot vertical dynamic is neglected, so the hypothesis that the normal force is always constant, the same for all the wheels and equal to the static value holds. Therefore, also all the inertial load transfer are neglected.

The longitudinal contact force f_{lonjk} is defined as a linear function of the wheel-contact plane relative velocity, while the lateral contact force f_{latjk} is a linear function of the lateral velocity of the wheel:

$$if\ \sqrt{f_{lonjk}^2 + f_{latjk}^2} \le \mu_s f_{njk} \quad \Rightarrow \quad \begin{cases} f_{lonjk} = k_{lonj}\left(r_{wj}\dot{\varphi}_{jk} - \dot{\rho}_{jk}\right) \\ f_{latjk} = -k_{latj}\dot{\eta}_{jk} \end{cases}$$

$$if\ \sqrt{f_{lonjk}^2 + f_{latjk}^2} > \mu_s f_{njk} \quad \Rightarrow \quad \begin{cases} f_{lonjk} = \mu_d f_{njk} \dfrac{k_{lonj}\left(r_{wj}\dot{\varphi}_{jk} - \dot{\rho}_{jk}\right)}{\sqrt{f_{lonjk}^2 + f_{latjk}^2}} \\ f_{latjk} = -\mu_d f_{njk} \dfrac{k_{latj}\dot{\eta}_{jk}}{\sqrt{f_{lonjk}^2 + f_{latjk}^2}} \end{cases} \tag{20}$$

3 Experimental validation

As said previously, some parameters must be identified in order to validate the proposed model correctly. The lateral and longitudinal wheel stiffness are the main parameters that need to be identified by fitting experimental data. In contrast, all the other model parameters can be easily measured or guessed with good approximation. The estimation process is done solving a non-linear least-square problem to minimise the difference between the measured quantities and the simulated states. This was performed using the Levenberg–Marquardt algorithm.

Different tests are done so that it is possible to isolate the effects of the parameters singularly in order to simplify the estimation of such parameters. The first set of tests consists of letting the robot move in a straight line at different velocities to estimate the parameters affecting the longitudinal dynamics without the influence of any lateral dynamics. In the second set of tests, instead, the robot follows a circular trajectory with different angular speeds to the right and left side. In these cases, both lateral and longitudinal dynamics are present, but with proper identification of the longitudinal ones, it is possible to focus on the estimation of lateral ones.

In all the tests, as many system states as possible have been measured. Modules poses and time derivatives have been measured using an image tracking system developed by the research group [18, 19], and the torque and the angular velocities of the active wheels have been measured with the robot sensors. Although all these tests were done using Epi.Q as a testing platform, the same methodology should also work for Agri.Q or any articulated robot that can be described by the model. The convenience of using Epi.Q is simply due to its limited size and manageable performance. It is also true that most of the inertial effects of the wheels are practically negligible with such a small robot, so the added complexity of the inertial effects should truly appear with a larger robot like Agri.Q.

The first set of tests consists of 7 different trials where the front module of the robot was set to reach and maintain the angular speeds of $100, 150, 200, 250, 300, 400$ and $500\ rad/s$ for the two motors driving the front wheels producing straight trajectories. From these tests, it is possible to identify the main parameters governing the longitudinal dynamics of the system: μ_s and μ_d , the contact static and dynamic friction coefficients, k_{lonj}, the longitudinal stiffness of the wheels, and k_{rollj}, the rolling friction parameter.

Fig. 4a depicts the comparison between the test with motors angular speed of $250\ rad/s$ and a simulation with the identified parameters; similar results are obtained for the other tests. The simulation slightly overshoots the experimental results for the slower speeds, while at higher speeds, they undershoot a little. However, in general, it is possible to state that the results are still a good representation of the tests.

Given the identified longitudinal parameters (Table 2), it is now easier to obtain an estimate for the wheels lateral stiffnesses k_{latj}, the main parameters governing the lateral dynamics of the articulated robot. However, even if the main focus here it is to estimate k_{latj}, all the previously identified parameters are estimated again, starting from the previous guesses. In order to achieve a good identification, a simple test was repeated two times to obtain some experimental data. In these tests, the motor on the right side was set to maintain $200\ rad/s$ while the left one had to keep the speed of $100\ rad/s$ for about one minute. With this set up, the robot follows a circular trajectory, whose radius should be about $0.445\ m$ if the motion is purely kinematic.

In Fig. 4b, it is possible to see the comparison of experimental and simulated results. Firstly, it has to be stated that the image-based tracking setup produces some uncertainty along the camera optical centre, for this reason, the experimental curve appears a little bit deformed in one direction, like an ellipse. However, it is possible to compute its mean radius, obtaining $0.441\ m$, so it is still close to the expected value. The average radius of the simulated trajectory, instead, is $0.466\ m$, so it can be considered a fine

approximation of the experimental results. Both the trajectories are pretty close to the ideal kinematic one, except during the initial straight transient.

Fig. 4(c-b) show the contact forces of the right and left front wheels. Here it is possible to see one of the limitations of the model: the hypothesis of a constant and equal vertical load on each wheel seems to lead to improper load distribution and consequently to wheel slip due to the strong correlation between vertical load and contact forces.

Table 2. Estimated parameters

Parameter	*Estimated value*	*Parameter*	*Estimated value*
μ_s	0.9	k_{rollj}	$8 \times 10^{-4} m$
μ_d	0.6	k_{latj}	$200\ Ns/m$
k_{lonj}	$120\ Ns/m$	k_{nj}	$11\ N/mm$

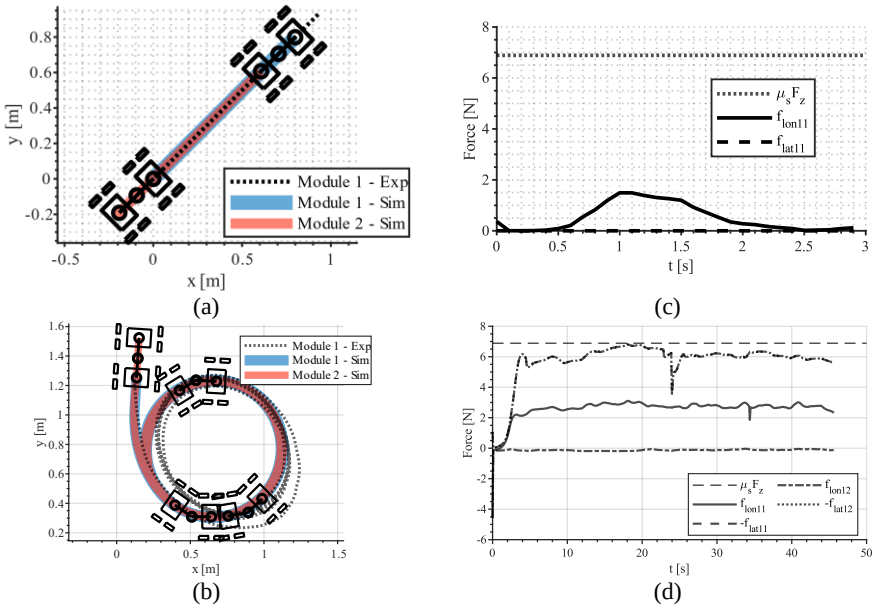

Fig. 4. (a-b) Comparison between the experimental and simulated trajectories. (c-d) Simulated front wheels contact forces.

4 Conclusions

In the present paper, a general dynamic model of articulated wheeled mobile robot subject to wheels slippage is modelled. The Newton-Euler method has been used to derive the system dynamic equations, and a very simple ground-wheel contact force model has been developed to represent wheels dynamics correctly. Some tests have been done

in order to estimate the model parameters governing the system longitudinal and lateral dynamics. By using these parameters, it has been possible to simulate with good precision the actual robot behaviour during straight and circular manoeuvres. However, it is already clear that further development of this model has to integrate some vertical dynamics too, due to their strong correlation to the contact forces.

This model provides a good starting point to develop some control architectures of autonomous articulated robots, in particular in case of also the second module is an active driving unit.

A similar identification methodology will be applied to Agri.Q, the larger agricultural rover, in order to verify the scalability of this model.

5 References

1. Dhaouadi R, Hatab AA (2013) Dynamic modelling of differential-drive mobile robots using lagrange and newton-euler methodologies: A unified framework. Advances in Robotics & Automation 2:1–7

2. Laumond J-P, Jacobs PE, Taix M, Murray RM (1994) A motion planner for nonholonomic mobile robots. IEEE Transactions on Robotics and Automation 10:577–593

3. He Y, Ren J (2013) A Comparative Study of Car-Trailer Dynamics Models. SAE International Journal of Passenger Cars-Mechanical Systems 6:177–186

4. Dragt BJ, Camisani-Calzolari FR, Craig IK (2005) MODELLING THE DYNAMICS OF A LOAD-HAUL-DUMP VEHICLE. IFAC Proceedings Volumes 38:49–54

5. Pradalier C, Usher K (2007) A simple and efficient control scheme to reverse a tractor-trailer system on a trajectory. In: Proceedings 2007 IEEE International Conference on Robotics and Automation. pp 2208–2214

6. Scheding S, Dissanayake G, Nebot EM, Durrant-Whyte H (1999) An experiment in autonomous navigation of an underground mining vehicle. IEEE Transactions on Robotics and Automation 15:85–95

7. Chen C, Tomizuka M (1997) Modeling And Control Of Articulated Vehicles.

8. Quaglia G, Cavallone P, Visconte C (2019) Agri_q: Agriculture UGV for Monitoring and Drone Landing. In: Gasparetto A, Ceccarelli M (eds) Mechanism Design for Robotics. Springer International Publishing, Cham, pp 413–423

9. Quaglia G, Visconte C, Scimmi LS, Melchiorre M, Cavallone P, Pastorelli S (2019) Design of the positioning mechanism of an unmanned ground vehicle for

precision agriculture. In: Uhl T (ed) Advances in Mechanism and Machine Science. Springer International Publishing, Cham, pp 3531–3540

10. Quaglia G, Visconte C, Scimmi LS, Melchiorre M, Cavallone P, Pastorelli S (2019) Robot arm and control architecture integration on a UGV for precision agriculture. In: Uhl T (ed) Advances in Mechanism and Machine Science. Springer International Publishing, Cham, pp 2339–2348

11. Quaglia G, Nisi M, Bruzzone L, Fanghella P (2017) Path Tracking Experimentation With Epi.q-Mod 2: An Obstacle Climbing Mobile Robot. https://doi.org/10.1115/IMECE2016-65838

12. Quaglia G, Nisi M (2016) Design and Construction of a New Version of the Epi.q UGV for Monitoring and Surveillance Tasks. https://doi.org/10.1115/IMECE2015-50163

13. Quaglia G, Butera LG, Chiapello E, Bruzzone L (2014) UGV Epi.q-Mod. In: Ceccarelli M, Glazunov VA (eds) Advances on Theory and Practice of Robots and Manipulators. Springer International Publishing, Cham, pp 331–339

14. Quaglia G, Oderio R, Bruzzone L, Razzoli R (2013) A modular approach for a family of ground mobile robots. International Journal of Advanced Robotic Systems 10:296

15. Bozzini G, Bruzzone L, Oderio R, Quaglia G, Razolli R (2009) Design of the small mobile robot Epi. q-2. Proceedings of AIMETA

16. Quaglia G, Cavallone P (2019) Rese_Q: UGV for Rescue Tasks Functional Design. https://doi.org/10.1115/IMECE2018-86395

17. Quaglia G, Cavallone P, Lenzo B (2019) On the Dynamic Analysis of a Novel Snake Robot: Preliminary Results. In: Carbone G, Gasparetto A (eds) Advances in Italian Mechanism Science. Springer International Publishing, Cham, pp 275–285

18. Botta A, Quaglia G (2019) Low-Cost Localization For Mobile Robot With Fiducial Markers. Proceedings of the 25th Chiefdom Symposium (2019) 2nd International Jc-IFToMM Symposium 26th October 2019, Kanagawa

19. Botta A, Quaglia G (SUBMITTED) Performance analysis of Low-cost tracking system for mobile robots. Machines - Selected Papers from Advances of Japanese Machine Design